Journal of Non-Crystalline Solids 626 (2024) 122806

Contents lists available at ScienceDirect

Journal of Non-Crystalline Solids

journal homepage: www.elsevier.com/locate/jnoncrysol

# A maximum temperature rise model of the shear band in bulk metallic glasses

Hao Zhang [a], Zhong Wang [b], Peter K. Liaw [c], Junwei Qiao [a,d,*], Yucheng Wu [d,e,*]

[a] College of Materials Science and Engineering, Taiyuan University of Technology, Taiyuan 030024, China
[b] College of Mechanical and Vehicle Engineering, Taiyuan University of Technology, Taiyuan 030024, China
[c] Department of Materials Science and Engineering, The University of Tennessee, Knoxville, TN 37996-2200, United States
[d] Key Laboratory of Interface Science and Engineering in Advanced Materials, Ministry of Education, Taiyuan University of Technology, Taiyuan 030024, China
[e] National-Local Joint Engineering Research Center of Nonferrous Metals and Processing Technology, Hefei University of Technology, Hefei 230009, China

ARTICLE INFO

*Keywords:*
Bulk metallic glasses
A maximum temperature rise model
A critical temperature

ABSTRACT

Based on mechanisms applicable to bulk metallic glasses (BMGs), such as a superposition principle of an instantaneous finite surface heat source temperature field and a flow model about the shear-band velocity, a maximum temperature rise model of shear bands in BMGs was deduced, $\Delta T_{\max} = \frac{\sigma_y}{c_p}\sqrt{\frac{\Delta t_{pl}\cdot v_{SB}}{2\pi\alpha}}$. The model describes the dependence of the maximum temperature rise on the yield strength and the shear-band velocity in BMGs. It can be calculated that the maximum temperature rise of BMGs is between 1 K ~ 30 K at room temperature through these two parameters. A critical temperature, $T_C$, of almost $0.8 \sim 0.9\ T_g$ is introduced, at $T < T_C$, the change of the yield strength with temperature in BMGs basically conforms a cooperative shear model (CSM), and at $T > T_C$, a significant reduction of the yield strength in BMGs can be attributed to avoiding failure due to localized material softening.

## 1. Introduction

Bulk metallic glasses (BMGs) are promising structural materials with extraordinary mechanical properties, including the high strength, large elastic strain, and significant fracture toughness, due to their long-range disordered structure [1–3]. However, nearly all plasticity is confined within nano-spanning shear bands, which leads to inhomogeneous plastic flows on the stress-strain curves [4,5] and usually results in catastrophic failure at low homologous temperatures ($T/T_g < 0.8$) [6]. Such a flow localization can be attributed to the thermal softening or mechanical softening, or a combination of both [7,8]. The temperature rise within shear bands in BMGs is a key factor in determining whether localized shear deformation and softening are stress or temperature driven [9].

The temperature rise within shear bands in BMGs has been studied by different measurements and modeling, including the fusible coating [10], infrared thermography [11], high-speed camera [12], thermo-mechanical simulator [13], and related theoretical studies [14–16]. These methods have shown that the temperature rise from less than 1 K [17] to several thousand Kelvin [10]. The reason for this huge difference is that the shear-band velocity or the shear-band duration is an important factor affecting the temperature rise within shear bands [18]. Different values of the shear-band duration, ranging widely from about 1 ns to few milliseconds, whose difference is as high as six orders of magnitude, have been reported by previous work [10,19]. Recently, a flow model accurately predicts the transition between the serrated and non-serrated flows in BMGs, and exactly provides equations for the shear band velocities of different BMGs which can be used in this work [20]. The aim of the present work is twofold: (1) to build a correlated model in exploring the temperature rise in BMGs by the shear-band velocity, and (2) to study the influence of the temperature rise on the yield strength of BMGs by the correlation model. Both (1) and (2) will contribute to a detailed understanding whether localized shear deformation and softening are stress or temperature driven in BMGs.

## 2. Theory

Georgarakis et al. [15] assumed that the shear band is approximated as an infinitely large plane with zero thickness, and the temperature rise can be calculated at a moment after shearing at a distance from the shear

* Corresponding authors.
*E-mail addresses:* qiaojunwei@gmail.com (J. Qiao), ycwu@hfut.edu.cn (Y. Wu).

https://doi.org/10.1016/j.jnoncrysol.2023.122806
Received 14 October 2023; Received in revised form 22 December 2023; Accepted 23 December 2023
Available online 28 December 2023

band based on the one-dimensional profile. The temperature rises have been proven to be very moderate during a stable serration flows by substituting the stress drop as a function of the time during a serration into the original constitutive equation of the temperature rise [21]. The maximum temperature jumps of 1 - 2 ℃ of an apparent band have been measured by time-resolved shear-band heating experiments. Using the experimental data by Luo et al. [22] for the compression of a $Zr_{52.5}Cu_{17.9}Ni_{14.6}Al_{10}Ti_5$ BMG (Vit 105) at a strain rate of $5 \times 10^{-4}\ s^{-1}$ and at room temperature. Fig. 1(a) shows a typical engineering stress-strain curve with serrated flows by the intermittent movement of the shear band. As shown in the left inset of Fig. 1(a), there is a close correspondent relation between the shear-band velocity (the displacement as a function of time) and corresponding stress drop as a function of the time [23]. Shear banding plays a key role in dominating the correspondence of BMGs during room-temperature compression. There is a sketch map, i.e., a major shear band is formed on a cuboid sample under the uniaxial compression, as shown in the right inset of Fig. 1(a). Fig. 1(b) is a schematic diagram where the shear band is considered as an instantaneous finite surface heat source that can be composed of multiple instantaneous point heat sources [15,24]. According to the solution of the temperature field by the superposition method of the heat source temperature field [24], the coordinate of the instantaneous point heat-source is ($x_i$, $y_i$, 0), and the coordinate position of any point, $M$, is ($x$, $y$, $z$), the temperature rise function is,

$$\theta = \frac{Q}{c_p(4\pi\alpha t)^{3/2}} e^{-\frac{(x-x_i)^2+(y-y_i)^2+z^2}{4\alpha t}}, \tag{1}$$

where $Q$ is the calorific value of the instantaneous point heat source, and $t$ is the time after the instantaneous point heat-source heats up instantaneously.

## 3. Calculation

Based on the superposition principle of the heat-source temperature field [24], a simple double integral method can be used to derive the calculated equation about the temperature field of the instantaneous finite surface-heat source. The temperature rise function of the major shear band, which is regarded as the instantaneous finite surface heat source, can be integrated for the point, $M$,

$$\theta_s = \int_0^B \mathrm{d}y_i \int_0^L \frac{Q_s}{c_p(4\pi\alpha t)^{3/2}} e^{-\frac{(x-x_i)^2+(y-y_i)^2+z^2}{4\alpha t}} \mathrm{d}x_i. \tag{2}$$

Thus, the calculated equation about the temperature field of the instantaneous finite surface heat-source is

$$\Delta T = \frac{Q_s C}{c_p(4\pi\alpha t)^{1/2}} e^{-\frac{z^2}{4\alpha t}}. \tag{3}$$

Compared with the calculated equation of the temperature field of an instantaneous infinite surface-heat source, Eq. (3) is only multiplied by a real coefficient, $C/4$, less than 1. The value of $C$ in the coefficient is,

$$\mathrm{C} = \left[\mathrm{erf}\left(\frac{x}{\sqrt{4\alpha t}}\right) - \mathrm{erf}\left(\frac{x-L}{\sqrt{4\alpha t}}\right)\right] \cdot \left[\mathrm{erf}\left(\frac{y}{\sqrt{4\alpha t}}\right) - \mathrm{erf}\left(\frac{y-B}{\sqrt{4\alpha t}}\right)\right]. \tag{4}$$

The effect of the size, the experimental temperature, and compositions of BMG samples on the value of $C$ is discussed deeply in the supplementary materials. The value of $C$ was determined to be 4 in BMGs for normal sample sizes at room temperature and above. Finally, the coefficient is chosen to be 1 for the shear band as the instantaneous finite surface-heat source. Zhang et al. [25] and Miracle et al. [16] calculated the temperature profiles around a shear band after the end of shearing in different BMGs, and exhibited that the maximum temperature rise occurs within the shear band. In this study, the temperature rise is only considered within the shear band, which is generated on the instantaneous finite surface heat source at $z = 0$. Therefore, the temperature rise of the shear band is

$$\Delta T = \frac{4Q_s}{c_p(4\pi\alpha t)^{1/2}}, \tag{5}$$

where $Q_s = 0.5\sigma_y \Delta u_{pl}$ is the heat flux of the shear band, $\sigma_y$ is the yield strength, $\Delta u_{\mathrm{pl}}$ is a given amplitude of the shear step of $\sim 1\ \mu m$, $\Delta u_{\mathrm{pl}}/\Delta t = 0.5 v_{\mathrm{SB}}$, $v_{SB}$ is the shear-band velocity, and $\Delta t$ is the time of shearing.

## 4. Results

So far, previous studies can be divided into two methods based on Eq. (5). Method I, the displacement burst size and the duration time can be gained through a scanning electron microscope and a high-speed camera during the propagation of shear-bands [26]. Method II, the local heating during the shear-band operation is measured with the fusible-coating method, rather than the temporal and the spatial resolution of conventional measurements [10]. The temperature-rise range within shear bands is estimated from less than 1 K [17] to several thousand Kelvin [10]. The main reason for the huge difference is that the duration of the shear-band operation cannot be described with a unified law. In other words, there is no universal model to describe the shear-band velocity of the entire plastic deformation dominated by shear bands during the uniaxial compression of BMGs. Thurnheer et al. [21] showed the temperature rise during stable plastic flows is very

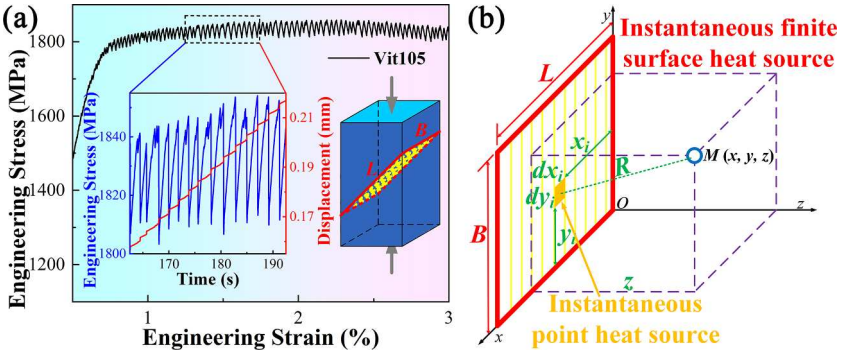


**Fig. 1.** (a) Typical engineering stress-strain curve with engineering strain of 0.5 - 3 % under the compression of a $Zr_{52.5}Cu_{17.9}Ni_{14.6}Al_{10}Ti_5$ BMG (Vit 105). The sample is a cylindrical with a diameter of 2 mm and the height of 4 mm. The left inset, a partial magnification of a black dotted box, shows the engineering stress (the blue curve) and the displacement (the red curve) as a function of the time. The right inset, a cuboid with 2 mm in the length and the width and 4 mm in the height, exhibits that a shear band with the length of L and the width of B is formed under compression. (b) The temperature field coordinates of the instantaneous finite surface heat source, which consists of the instantaneous point heat source. Here, the shear band in the shearing process is regarded as the instantaneous finite surface heat source.

moderate by converting the shear-band velocity to the stress drop as a function of the time and substituting it into Eq. (5). The relation is $\Delta u_{\rm pl} = \sqrt{2}\Delta F(C_M + C_S)$, where $\Delta F/A = \Delta\sigma$, $\Delta F$ is the load drop, $A$ is the cross-sectional area, $\Delta\sigma$ is the stress drop, $C_M$ is the machine compliance, and $C_S$ is the sample compliance. Before, we developed a flow model in metallic glasses, which describes the shear-band velocity during serrated flows [20]. Therefore, the shear-band velocity can be directly substituted into Eq. (5). Meanwhile, the maximum temperature rise, $\Delta T_{\max}$, occurs at the latest moment of the shearing. Substituting $t = \Delta t$ into Eq. (5) gives a maximum temperature rise model as

$$\Delta T_{\max} = \frac{\sigma_y}{c_p}\sqrt{\frac{\Delta u_{pl}\cdot v_{SB}}{2\pi\alpha}}, \tag{6}$$

where $c_p \approx 3\times10^6 J\ m^{-3}\ K^{-1}$ is the specific volume heat capacity of BMGs, and $\alpha \approx 2\times10^{-6} m^2\ s^{-1}$ is the thermal diffusivity of BMGs [15].

The shear-band velocities and the yield strengths of twelve BMGs were summarized at room temperature [20,27], and $\Delta T_{\max}$ of these BMGs was calculated by Eq. (6), as listed in Table 1. Fig. 2 is a three-dimensional coordinate diagram, where $v_{SB}$ is the x axis, $\sigma_y$ is the y axis, and $\Delta T_{\max}$ is the z axis. The two longitudinal planes in Fig. 2 are the relationship between $\Delta T_{\max}$ and $v_{SB}$ or $\sigma_y$, respectively. $\Delta T_{\max}$ of these BMGs increases with increasing the shear-band velocity, which shows a strong correlation, and conversely, $\sigma_y$ can be considered as a coefficient from $\Delta T_{\max}$ equation. It can be concluded that $\Delta T_{\max}$ of these BMGs is between 1 ~ 30 K at room temperature and half of these BMGs have $\Delta T_{\max}$ of 1 ~ 3 K at room temperature. Taking the $Zr_{65}Co_{25}Al_{10}$ and $Zr_{65}Cu_{15}Al_{10}Ni_{10}$ BMGs as examples, the model indicates that their maximum temperatures rise at room temperature are 1.88 K and 2.51 K, respectively. Thurnheer et al. [21] obtained that $\Delta T_{\max}$ of the $Zr_{57.1}Co_{28.6}Al_{14.3}$ BMG was about 1.9 K through experimental measurements and related model analysis at room temperature. Li et al. [28] considered the effects of the strain rates and machine stiffness, which was taken into account in the experiments and calculations, and concluded that $\Delta T_{\max}$ of the $Zr_{62}Cu_{15.5}Ni_{12.5}Al_{10}$ BMG was about 2.5 K at room temperature. Therefore, the model has general applicability in predicting $\Delta T_{\max}$ within shear bands at room temperature.

## 5. Discussion

According to the flow model [20], the shear-band velocity of the BMGs is related to its activation energy, $E_S$, and experimental temperature, $T$, as $v_{SB} = \nu_0 a_0 \cdot \exp(E_S/kT_1 - E_S/kT)$. For a BMG, $E_S$ is basically constant. Hence, its shear-band velocity increases with increasing $T$. Combining with Eq. (6), the parameters are basically constant in a certain experimental temperature range except $v_{SB}$. Hence, $\Delta T_{\max}$ of the BMG increases with the increase of $T$. Spaepen [29] found that the yield strengths of BMGs with main components of Pd and Si remained unchanged in a large experimental temperature range far below $T_g$, and the yield strength of these BMGs dropped significantly in a small experimental temperature range close to $T_g$. In order to explain this phenomenon, Spaepen pictured a schematic deformation diagram of BMGs to indicate the various deformation modes and proposed that the materials can be called 'viscous' when $T \approx T_g$, and the materials may be called 'solid' when $T \ll T_g$. Here, $T_g$ is considered as a transition point from the 'solid' to the 'viscous.' A critical temperature, $T_C$, is defined, and the sum of $\Delta T_{\max}$ at $T_C$ and $T_C$ is equal to $T_g$,

$$\Delta T_{\max}(T_C) + T_C = T_g. \tag{7}$$

$T_g$ and the equations from $v_{SB}$ of twelve BMGs were summarized [20,30], and $T_C$ was calculated by Eq. (7), and $T_C/T_g$ of these BMGs was determined, as listed in Table 2. Fig. 3 exhibits the sum of the maximum temperature rise and the experimental temperature, $\Delta T_{\max}(T) + T$, of twelve BMGs is plotted as a function of $T$, and the horizontal and vertical coordinates are normalized by $T_g$. The inset in Fig. 3 is the variation of $\Delta T_{\max}$ with $T$, and the abscissa cuts off at $T_C$. The values of $T_C$ of these BMGs are scattered in the range of 350 ~ 750 K. In comparison, the values of $T_C/T_g$ of these BMGs are uniformly distributed within 0.8 ~ 0.9, except for the $La_{57.5}Al_{15}Cu_{27.5}$ BMG, in which $\Delta T_{\max}$ is less than 30 K at $T_C$. Similarly, $\Delta T_{\max}$ of these BMGs at $T_C$ is scattered in the range of 25 - 165 K, and the ratio of $\Delta T_{\max}$ at $T_C$ to $T_g$ of these BMGs is uniformly distributed within 0.1 - 0.2, except for the $La_{57.5}Al_{15}Cu_{27.5}$ BMG. Li et al. [31] summarized the change of the normalized strength, $\sigma_y/E$, with the normalized temperature, $T/T_g$, at similar strain rates for four BMGs with different compositions, and found that there are two very different linear relationships between $\sigma_y/E$ and $T/T_g$ before and after 0.9 $T_g$. Before 0.9 $T_g$, $\sigma_y/E$ remained basically unchanged with the increase of $T/T_g$, with a slope of - 0.0106; after 0.9 $T_g$, $\sigma_y/E$ decreased suddenly with the increase of $T/T_g$, with a slope of - 0.117. Tong et al. [32] have indicated that annealing at 0.8 ~ 0.9 $T_g$ generally leads to the structural relaxation with the unchanged yield strength, and severe brittleness because of the increased resistance for the nucleation of shear bands. When the experimental temperature is greater than 0.9 $T_g$, and the yield strength remains unchanged, the temperature within shear bands will be greater than $T_g$ according to Eq. (6). Hence, the shear band softens, and catastrophic failure occurs. Therefore, the sudden decrease of $\sigma_y/E$ of BMGs can be attributed to avoiding the catastrophic destruction of the shear-band softening when the experimental temperature is greater than 0.9 $T_g$.

The 0.2 % yield stress and the maximum stress at different temperatures under quasi-static compression for the $Pd_{77.5}Cu_6Si_{16.5}$ BMG given by Pampillo and Chen [33] and $Zr_{52.5}Cu_{17.9}Ni_{14.6}Al_{10}Ti_5$ BMG given by Dubach et al. [34], as presented in Fig. 4. Pampillo and Chen found that the yield strength of the $Pd_{77.5}Cu_6Si_{16.5}$ BMG decreases rapidly at about 530 K, and the temperature is about 116 K lower than $T_g$ of the BMG (646 K) measured by Chen and Turnbull [35], but the temperature is very close to the $T_C$ of the $Pd_{78}Cu_6Si_{16}$ BMG (546 K) calculated by Eq. (7). Dubach et al. measured more data points with a larger temperature range in this series of experiments, and detected a clear deviation from the $T^{2/3}$-law proposed for BMGs by Johnson and Samwer [36]. The authors observe that the maximum stress of the $Zr_{52.5}Cu_{17.9}Ni_{14.6}Al_{10}Ti_5$ BMG decreases rapidly at about 575 K, and the temperature is closer to the $T_C$ of the BMG (572 K) calculated by Eq. (7) and is about 105 K lower than $T_g$ of the BMG (680 K). A cooperative shear model (CSM) for plastic yielding of BMGs, $\tau_Y/G = \gamma_{C0} - \gamma_{C1}(T/T_g)^m$ with $\tau_Y = \sigma_Y/2$, is fully applicable to the data points for two BMGs before $T_C$ [36]. For the $Zr_{52.5}Cu_{17.9}Ni_{14.6}Al_{10}Ti_5$ BMG with $G = 32.3$ GPa, $\gamma_{C0} = 0.038$, $\gamma_{C1} = 0.014$, $m = 0.485$, and the fitting degree is $R^2 = 0.93$. All fitting parameters of the BMG conform to the CSM. For the $Pd_{77.5}Cu_6Si_{16.5}$ BMG with $G = 32.9$ GPa, $\gamma_{C0} = 0.034$, $\gamma_{C1} = 0.014$, $m = 0.325$, and the fitting degree is $R^2 = 0.90$. The values of $\gamma_{C0}$ and $\gamma_{C1}$ of the BMG all meet the CSM, but the value of $m$ of the BMG deviates slightly from the CSM to obtain a higher fitting degree. Fortunately, the same data points of the BMG were perfectly fitted in the CSM, as shown the vertical triangle of

**Table 1**
For various BMGs: the shear-band velocity, $v_{SB}$, at room temperature [20]; the yield strength, $\sigma_y$, at room temperature [27]; the maximum temperature rise, $\Delta T_{\max}$, at room temperature.

| | $v_{SB}$(mm/s) | $\sigma_y$(MPa) | $\Delta T_{\max}$(K) |
|---|---|---|---|
| $Au_{49}Cu_{26.9}Ag_{5.5}Pd_{2.3}Si_{16.3}$ | 56.66 | 1.32 | 29.54 |
| $Zr_{52.5}Cu_{17.9}Ni_{14.6}Al_{10}Ti_5$ | 1.05 | 1.8 | 5.49 |
| $Pt_{57.5}Cu_{14.7}Ni_{5.3}P_{22.5}$ | 0.27 | 1.4 | 2.18 |
| $Zr_{65}Cu_{15}Al_{10}Ni_{10}$ | 0.34 | 1.45 | 2.51 |
| $Cu_{60}Zr_{20}Hf_{10}Ti_{10}$ | 10.08 | 1.95 | 18.41 |
| $Fe_8Ni_{70}Si_{10}B_{12}$ | 0.06 | 3.6 | 2.56 |
| $La_{57.5}Al_{15}Cu_{27.5}$ | 42.31 | 0.64 | 12.38 |
| $Zr_{45}Cu_{45}Al_{10}$ | 8.93 | 1.95 | 17.32 |
| $Zr_{65}Co_{25}Al_{10}$ | 0.14 | 1.7 | 1.88 |
| $Co_{78}Si_{10}B_{12}$ | 0.01 | 3.45 | 1.14 |
| $Pd_{78}Cu_6Si_{16}$ | 0.73 | 1.57 | 3.98 |
| $Ni_{62}Nb_{38}$ | 0.09 | 3.2 | 2.80 |

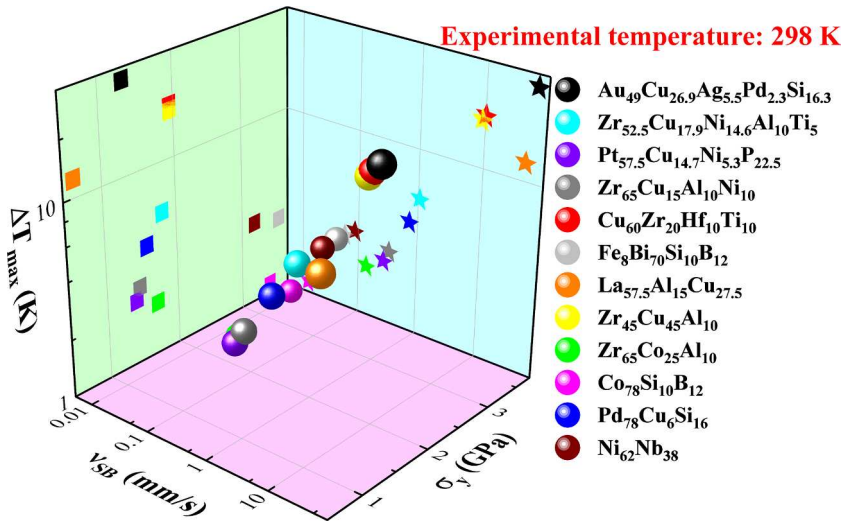


**Fig. 2.** The three-dimensional coordinate diagram of the yield strength, $\sigma_y$, the shear-band velocity, $v_{SB}$, and the maximum temperature rise, $\Delta T_{max}$, of different BMGs at the experimental temperature of 298 K.

**Table 2**
For various BMGs: the shear-band velocity as a function of the temperature, $v_{SB}(T)$ [20]; the glass transition temperature, $T_g$ [30]; the critical temperature, $T_C$; the ratio of $T_C$ to $T_g$, $T_C/T_g$.

| | $v_{SB}(T)$(mm/s) | $T_g$(K) | $T_C$(K) | $T_C/T_g$ |
|---|---|---|---|---|
| $Au_{49}Cu_{26.9}Ag_{5.5}Pd_{2.3}Si_{16.3}$ | 10^(4.864–927/T) | 401 | 350 | 0.87 |
| $Zr_{52.5}Cu_{17.9}Ni_{14.6}Al_{10}Ti_5$ | 10^(5.424–1610/T) | 680 | 572 | 0.84 |
| $Pt_{57.5}Cu_{14.7}Ni_{5.3}P_{22.5}$ | 10^(8.165–2601/T) | 502 | 443 | 0.88 |
| $Zr_{65}Cu_{15}Al_{10}Ni_{10}$ | 10^(5.44–1761/T) | 670 | 595 | 0.89 |
| $Cu_{60}Zr_{20}Hf_{10}Ti_{10}$ | 10^(4.611–1075/T) | 722 | 582 | 0.81 |
| $Fe_8Ni_{70}Si_{10}B_{12}$ | 10^(4.652–1757/T) | 755 | 653 | 0.86 |
| $La_{57.5}Al_{15}Cu_{27.5}$ | 10^(4.915–980/T) | 402 | 375 | 0.93 |
| $Zr_{45}Cu_{45}Al_{10}$ | 10^(4.699–1117/T) | 710 | 573 | 0.81 |
| $Zr_{65}Co_{25}Al_{10}$ | 10^(5.188–1802/T) | 688 | 619 | 0.90 |
| $Co_{78}Si_{10}B_{12}$ | 10^(4.871–2020/T) | 800 | 699 | 0.87 |
| $Pd_{78}Cu_6Si_{16}$ | 10^(5.503–1681/T) | 622 | 546 | 0.88 |
| $Ni_{62}Nb_{38}$ | 10^(4.869–1768/T) | 892 | 732 | 0.82 |

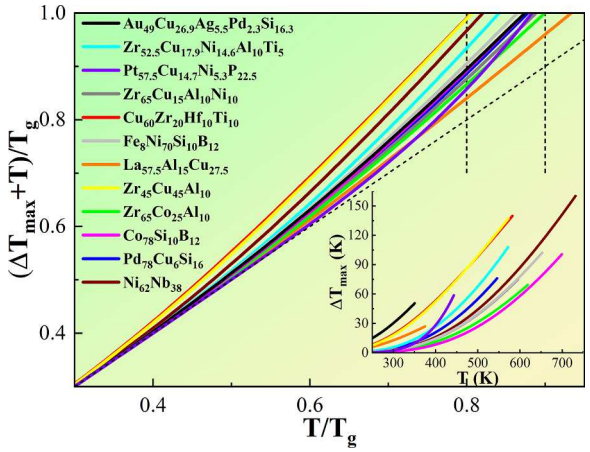


**Fig. 3.** The experimental temperature plus the maximum temperature rise as a function of the experimental temperature is plotted for all BMGs mentioned in Fig. 2., and the horizontal and vertical coordinates are scaled to the glass transition temperature, $T_g$. The specific temperature-rise changes of these BMGs are shown in the inset, and the cut-off points of the abscissa are the critical experimental temperature, $T_C$, for these BMGs.

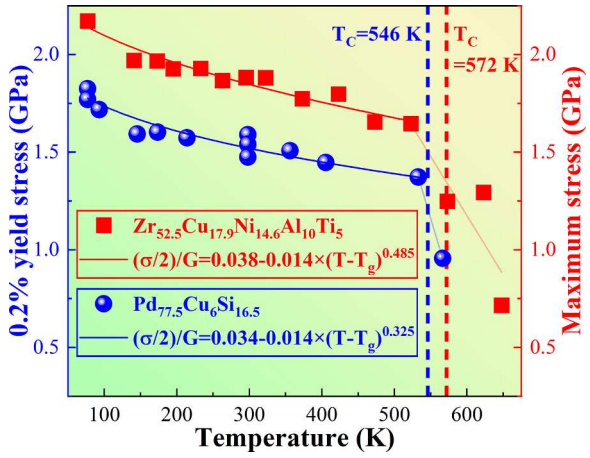


**Fig. 4.** The 0.2 % yield stress at different temperatures under quasi-static compression for the $Pd_{77.5}Cu_6Si_{16.5}$ BMG given by Pampillo and Chen [33]. And the maximum stress at different temperatures under quasi-static compression for the $Zr_{52.5}Cu_{17.9}Ni_{14.6}Al_{10}Ti_5$ BMG given by Dubach et al. [34]. The abscissas corresponding to the red and blue dotted lines are the critical temperature, $T_C$, of the two BMGs, respectively. According to the CSM, the fitting curves of the data points before $T_C$ for the Zr-based BMG and the Pd-based BMG are $(\sigma/2)/G = 0.038 - 0.014 \times (T - T_g)^{0.485}$ with $R^2 = 0.93$ of the fitting degree and $(\sigma/2)/G = 0.034 - 0.014 \times (T - T_g)^{0.325}$ with $R^2 = 0.90$ of the fitting degree, respectively.

Fig. 2 in Ref. [36]. In summary, it can be concluded that at $T < T_C$, the change of the yield strength with temperature in BMGs basically conforms the CSM, and at $T > T_C$, the significant reduction of the yield strength in BMGs can be attributed to avoiding failure due to localized material softening.

## 6. Conclusions

In this study, the maximum temperature rise model of shear bands in BMGs was established through mechanisms applicable to BMGs, such as the superposition principle of the instantaneous finite surface heat source temperature field and the flow model about the shear-band velocity in BMGs. The model was deduced through rigorous processes, $\Delta T_{max} = \frac{\sigma_y}{c_p}\sqrt{\frac{\Delta t_{pl} \cdot v_{SB}}{2\pi\alpha}}$, which describes the dependence of the maximum

temperature rise on the yield strength and the shear-band velocity in BMGs. Compared with the experimental data reported from the previous work, the current model can accurately predict the maximum temperature rise of BMGs at room temperature. Combining with the yield strength and the shear-band velocity of many BMGs, it can be concluded that the maximum temperature rise of BMGs is between 1 K ~ 30 K at room temperature. The shear-band velocity increases with the increased experimental temperature in the flow model. Hence, the maximum temperature rise also increases with the increase of the experimental temperature. The critical temperature, $T_C$, is introduced that comprehensively explains the variation of the yield strength with temperature. At $T < T_C$, the CSM is basically suitable for the change of the yield strength with temperature, and at $T > T_C$, the significant reduction of the yield strength in BMGs can be attributed to avoiding failure due to localized material softening.

## CRediT authorship contribution statement

**Hao Zhang:** Writing – review & editing, Writing – original draft, Visualization, Validation, Software, Resources, Methodology, Investigation, Formal analysis, Data curation, Conceptualization. **Zhong Wang:** Validation, Project administration, Funding acquisition. **Peter K. Liaw:** Writing – review & editing, Validation, Funding acquisition. **Junwei Qiao:** Writing – review & editing, Visualization, Validation, Supervision, Methodology, Investigation, Funding acquisition, Formal analysis. **Yucheng Wu:** Writing – review & editing, Validation, Project administration, Formal analysis.

## Declaration of Competing Interest

The authors declare that they have no known competing financial interests or personal relationships that could have appeared to influence the work reported in this paper.

## Data availability

Data will be made available on request.

## Acknowledgment

J.W.Q. would like to acknowledge the financial support of the National Natural Science Foundation of China (No. 52071229). Z.W. would like to acknowledge the financial support of the National Natural Science Foundation of China (No. 52201188), and the Research Project of Shanxi Scholarship Council of China (No. 2022-037). P.K.L. very much appreciates the support from the National Science Foundation (DMR – 1611180, 1809640, and 2226508).

## References

[1] M.M. Trexler, N.N. Thadhani, Mechanical properties of bulk metallic glasses, Prog. Mater. Sci. 55 (2010) 759–839.
[2] C. Schuh, T. Hufnagel, U. Ramamurty, Mechanical behavior of amorphous alloys, Acta Mater. 55 (2007) 4067–4109.
[3] B.A. Sun, W.H. Wang, The fracture of bulk metallic glasses, Prog. Mater. Sci. 74 (2015) 211–307.
[4] J. Antonaglia, W.J. Wright, X. Gu, R.R. Byer, T.C. Hufnagel, M. LeBlanc, J.T. Uhl, K. A. Dahmen, Bulk metallic glasses deform via slip avalanches, Phys. Rev. Lett. 112 (2014), 155501.
[5] W. Jiang, G. Fan, F. Liu, G. Wang, H. Choo, P. Liaw, Spatiotemporally inhomogeneous plastic flow of a bulk-metallic glass, Int. J. Plast. 24 (2008) 1–16.
[6] L.A. Davis, Y.T. Yeow, Flow and fracture of a Ni-Fe metallic glass, J. Mater. Sci. 15 (1980) 230–236.
[7] W.J. Wright, R.B. Schwarz, W.D. Nix, Localized heating during serrated plastic flow in bulk metallic glasses, Mater. Sci. Eng. A 319–321 (2001) 229–232.
[8] Y.Q. Cheng, Z. Han, Y. Li, E. Ma, Cold versus hot shear banding in bulk metallic glass, Phys. Rev. B 80 (2009) 134115.
[9] S.V. Ketov, D.V. Louzguine-Luzgin, Localized shear deformation and softening of bulk metallic glass: stress or temperature driven? Sci. Rep. 3 (2013) 2798.
[10] J.J. Lewandowski, A.L. Greer, Temperature rise at shear bands in metallic glasses, Nat. Mater. 5 (2005) 15–18.
[11] G. Wang, Q. Feng, B. Yang, W. Jiang, P.K. Liaw, C.T. Liu, Thermographic studies of temperature evolutions in bulk metallic glasses: an overview, Intermetallics 30 (2012) 1–11.
[12] Y. Yokoyama, H. Tokunaga, A.R. Yavari, M. Yamada, T. Yamasaki, K. Fujita, A. Inoue, Viscous flow in sliding shear band formed during tensile deformation of hypoeutectic Zr-based metallic glass, Intermetallics 19 (2011) 1683–1687.
[13] S.-H. Joo, H. Kato, K. Gangwar, S. Lee, H.S. Kim, Shear banding behavior and fracture mechanisms of Zr55Al10Ni5Cu30 bulk metallic glass in uniaxial compression analyzed using a digital image correlation method, Intermetallics 32 (2013) 21–29.
[14] J.G. Wang, Y. Pan, S.X. Song, B.A. Sun, G. Wang, Q.J. Zhai, K.C. Chan, W.H. Wang, How hot is a shear band in a metallic glass? Mater. Sci. Eng. A 651 (2016) 321–331.
[15] K. Georgarakis, M. Aljerf, Y. Li, A. LeMoulec, F. Charlot, A.R. Yavari, K. Chornokhvostenko, E. Tabachnikova, G.A. Evangelakis, D.B. Miracle, A.L. Greer, T. Zhang, Shear band melting and serrated flow in metallic glasses, Appl. Phys. Lett. 93 (2008), 031907.
[16] D.B. Miracle, A. Concustell, Y. Zhang, A.R. Yavari, A.L. Greer, Shear bands in metallic glasses: size effects on thermal profiles, Acta Mater. 59 (2011) 2831–2840.
[17] B. Yang, P.K. Liaw, G. Wang, M. Morrison, C.T. Liu, R.A. Buchanan, Y. Yokoyama, In-situ thermographic observation of mechanical damage in bulk-metallic glasses during fatigue and tensile experiments, Intermetallics 12 (2004) 1265–1274.
[18] M.T. Asadi Khanouki, Temperature rise in shear bands and its effect on crystallization behavior in bulk metallic glasses, J. Alloys Compd. 936 (2023), 168198.
[19] S.X. Song, T.G. Nieh, Flow serration and shear-band viscosity during inhomogeneous deformation of a Zr-based bulk metallic glass, Intermetallics 17 (2009) 762–767.
[20] H. Zhang, Z. Wang, H.J. Yang, X.H. Shi, P.K. Liaw, J.W. Qiao, A flow model in bulk metallic glasses, Scr. Mater. 222 (2023), 115047.
[21] P. Thurnheer, F. Haag, J.F. Löffler, Time-resolved measurement of shear-band temperature during serrated flow in a Zr-based metallic glass, Acta Mater. 115 (2016) 468–474.
[22] Y.S. Luo, Z. Wang, J. Eckert, J.W. Qiao, A universal criterion for the failure threshold in slowly sheared bulk metallic glasses, J. Appl. Phys. 129 (2021), 155109.
[23] R. Maaß, J.F. Löffler, Shear-band dynamics in metallic glasses, Adv. Funct. Mater. 25 (2015) 2353–2368.
[24] H.S. Carslaw, J.C. Jaeger, Conduction of Heat in Solids, Oxford University Press, 1959 second ed.
[25] Y. Zhang, N.A. Stelmashenko, Z.H. Barber, W.H. Wang, J.J. Lewandowski, A. L. Greer, Local temperature rises during mechanical testing of metallic glasses, J. Mater. Res. 22 (2011) 419–427.
[26] S.X. Song, X.L. Wang, T.G. Nieh, Capturing shear band propagation in a Zr-based metallic glass using a high-speed camera, Scr. Mater. 62 (2010) 847–850.
[27] Z.Q. Liu, Z.F. Zhang, Strengthening and toughening metallic glasses: the elastic perspectives and opportunities, J. Appl. Phys. 115 (2014) 163505.
[28] J.J. Li, J.F. Fan, Z. Wang, Y.C. Wu, K.A. Dahmen, J.W. Qiao, Temperature rises during strain-rate dependent avalanches in bulk metallic glasses, Intermetallics 116 (2020), 106637.
[29] F. Spaepen, A microscopic mechanism for steady state inhomogeneous flow in metallic glasses, Acta Metall. 25 (1977) 407–415.
[30] R.T. Qu, Z.Q. Liu, R.F. Wang, Z.F. Zhang, Yield strength and yield strain of metallic glasses and their correlations with glass transition temperature, J. Alloys Compd. 637 (2015) 44–54.
[31] H. Li, C. Fan, K. Tao, H. Choo, P.K. Liaw, Compressive behavior of a Zr-based metallic glass at cryogenic temperatures, Adv. Mater. 18 (2006) 752–754.
[32] Y. Tong, W. Dmowski, Y. Yokoyama, G. Wang, P.K. Liaw, T. Egami, Recovering compressive plasticity of bulk metallic glasses by high-temperature creep, Scr. Mater. 69 (2013) 570–573.
[33] C.A. Pampillo, H.S. Chen, Comprehensive plastic deformation of a bulk metallic glass, Mater. Sci. Eng. 13 (1974) 181–188.
[34] A. Dubach, F. Dallatorre, J. Loffler, Constitutive model for inhomogeneous flow in bulk metallic glasses, Acta Mater. 57 (2009) 881–892.
[35] H.S. Chen, D. Turnbull, Formation, stability and structure of palladium-silicon based alloy glasses, Acta Metall. 17 (1969) 1021–1031.
[36] W.L. Johnson, K. Samwer, A universal criterion for plastic yielding of metallic glasses with a $(T/T_g)^{2/3}$ temperature dependence, Phys. Rev. Lett. 95 (2005), 195501.